Intelligent Pupil Technology Applied on TMA System on Space-Borne Camera

Yan Feng

Key Laboratory of Optical System Advanced Manufacturing Technology, Changchun Institute of Optics, Fine Mechanics and Physics, Chinese Academy of Sciences, Changchun, Jilin 130033, *China*

Abstract The off-axis three mirror anastigmatic (TMA) system has been proven a sort of excellent optical system for space-borne camera especially the compact cameras because of its high modulation transfer function (MTF) and large field-of-view (FOV). Several new methods that can be applied on the space-borne TMA system are proposed to improve its performance. Because all the improvement is realized by manipulating the pupil function indirectly, these new methods are jointly called intelligent pupil technology.

Key words imaging systems; intelligent pupil, wavefront coding, deformable mirror, phase diversity

OCIS codes 110.1758; 100.5070; 110.6770; 220.1080; 220.4830

应用于TMA系统的智能光瞳技术

闫 锋

中国科学院长春光学精密机械与物理研究所光学系统先进制造技术重点实验室,吉林 长春 130033

摘要 离轴三反消像散(TMA)光学系统由于可以同时实现长焦距和大视场,被认为是新一代空间光学系统、尤其是紧凑型系统的首选。为提高系统性能,提出了通过调制出瞳函数改善系统质量的智能光瞳技术,包括波前编码、相位参差以及主动变形镜技术。针对某TMA系统,详细介绍了应用波前编码技术的系统设计结果、应用相位参差技术的波前探测及应用主动变形镜的波前校正实验。实验结果表明,智能光瞳技术的应用确实可以提升系统质量。

关键词 成像系统;智能光瞳;波前编码;变形镜;相位参差

中图分类号 O439 **文献标识码** A **doi**: 10.3788/LOP51.051101

1 Introduction

Our research is based on a typical Cook′s three-mirror anastigmatic (TMA) system (invented by Wetherell *et al.*) [1] for compact space-borne camera. This kind of TMA system has two distinct characteristics: the one is that the exit pupil is virtual because the aperture stop is located at the position of secondary mirror, which means that there is no real light passes through the exit pupil; and the other is the size of secondary mirror which much smaller than primary mirror (PM) and tertiary mirror (TM). Thus it can be concluded that it is impossible to improve the system′s performance by means of appending extra optical components at the position of exit pupil, but the improvement can be achieved through manipulating the pupil function by transforming the surface figure of the secondary mirror since it serves as the aperture stop. Furthermore, it is not so difficult to manufacture unusual surface figure on the secondary mirror for its relatively small size. Because all the improvement is carried out related to the pupil function, it is called intelligent pupil technology as a general name. The dynamic image quality can be improved by wavefront error testing and correcting based on intelligent pupil technology, especially when there is a sudden change or disturbance happening to the telescope.

收稿日期: 2013-10-09; **收到修改稿日期**:2013-12-12; **网络出版日期**: 2014-04-30

基金项目: 国家自然科学基金重点项目(61036015)

作者简介: 闫 锋(1981—),博士,副研究员,主要从事波前编码技术、光学系统检测等方面的研究。

E-mail: yanfeng@ciomp.ac.cn

The intelligent pupil technology can enable the telescope more responsibility to these external disturbance or make the telescope less sensitive to some error source.

2 Wavefront coding technology

As known, it is difficult to maintain the focal plane position of a space-borne camera within its depth of focus (DOF) because of long-distance transport, launch shock and thermal loading in orbit. Wavefront coding technology (WFC) provides a new feasible way to solve these problems, which is an innovative system-level technology that can control misfocus-related aberrations including misfocus, astigmatism and Petzval curvature, as well as temperature-related and alignment-related misfocus in digital imaging systems. It has been applied in bar- code scanning system, iris- recognizing system, mobile camera, biology microscope, infrared monitoring system, folded telescope, and so on[2-7]. According to this technology, if a special phase distribution is appended to a common pupil function, image quality will nearly remain the same within a wide range larger than 10 times DOF of original system. Of course the medial image will be degraded, but it can be easily restored by post-processing because the additive phase is completely known ahead. The usual form of the extra phase added to pupil function is the cubic term:

$$P(x,y)=\frac{1}{\sqrt{2}}\exp[\mathrm{j}\alpha(x^3+y^3)],\quad |x|\leqslant 1,\ |y|\leqslant 1, \tag{1}$$

where (x,y) is the normalized coordinate. This phase distribution can be introduced by adding a proper cubic term to the surface figure of the secondary mirror as

$$z(x,y)=\frac{c(x^2+y^2)}{1+\sqrt{1-(1+k)c^2(x^2+y^2)}}+\beta(x^3+y^3), \tag{2}$$

where c is the reciprocal of the vertex curvature radius and k is the conic.

Of course the determination of β value is achieved through an effective model according to the system parameter. It can be observed in Fig.1 that the modulation transfer function (MTF) curves of an arbitrary field- of- view (FOV) coincides with each other perfectly while MTF curves of traditional system show notable distinction when the defocus aberration varies from -1.25λ to 1.25λ with λ being the light wavelength. It can be validated that the MTF curves of any FOV are provided with fine uniformity although they are not shown for concision. The DOF of the system can be regarded as being extended as 10 times as before.

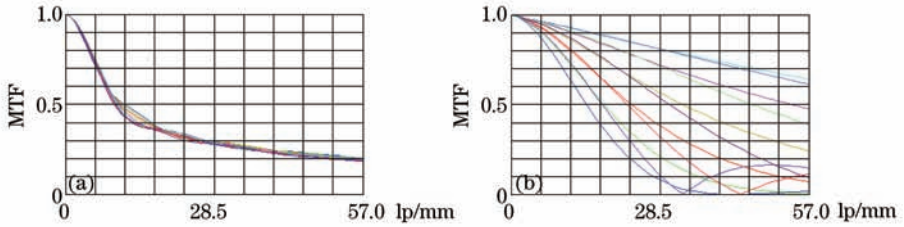

Fig.1 Comparison of MTF curves between (a) wavefront coded system and (b) traditional system when the defocus aberration varies from -1.25λ to 1.25λ

3 Phase diversity technology

Even though the atmosphere turbulence effects can be neglected, the images of space- borne cameras will also be degraded by their own fixed aberration originating from residual errors of fabrication and alignment, various thermal and mechanical stresses, vibrations and other unforeseen aspects. The detailed information and exact character of the aberration are necessary in the post-processing of remote sensing images. The phase diversity (PD) technology is regarded as a powerful candidate for aberration sensing of space telescope. This kind of metrology needs a set of images collected simultaneously, each of which is formed via a slightly different pupil phase screen. PD technology is applied to measure the piston error among different segments of the primary mirror of Keck II telescope by Lockheed Martin Space Systems. Boeing Company and General Dynamic also have built the experimental platform to validate the technology[8-12]. The typical schematic is shown in Fig.2.

In PD technology, the defocused image is considered to be the "diversity" image and the defocus value is set artificially. The aberration of the system can be calculated by minimizing certain appropriate cost function deduced by the two images. But this scheme is rather difficult to realize in the TMA system under research. The image plane of the TMA system under research is comprised of five pieces of time

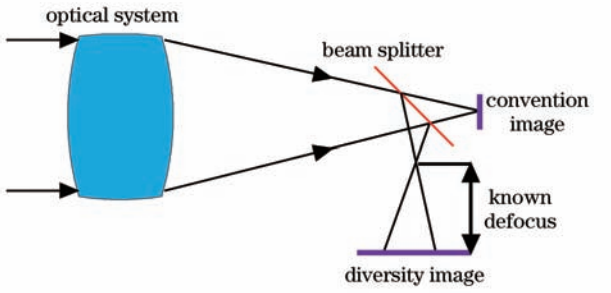

Fig.2 Typical schematic setup of PD technology

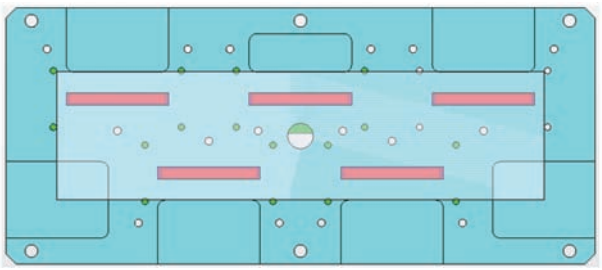

Fig.3 Original image plane

delay integrated (TDI) CCD array stitched together, as shown in Fig.3.

If a beam splitter is used, its size will be at least larger than 240 mm×50 mm. It will be of great mechanical difficulty to hold so big a component steadily and accurately in front of the image plane within such a narrow space. The other fatal problem is that there is no free space for the defocused image plane. Considering that the working mode of the camera is push-broom and the same object will be imaged by each line of CCD array, the "diversity" images can be obtained by enlarging the effective FOV in its scanning direction and increasing the lines of CCD array.

Based on the original system, totally 21 Zernike polynomial terms are added to the original surface figure of the secondary mirror, which helps to correct the residual off-axis and high-order aberration[13-14]:

$$z(x,y)=\frac{c(x^2+y^2)}{1+\sqrt{1-(1+k)c^2(x^2+y^2)}}+\sum_{i=5}^{25}A_iZ_i(x,y)\,, \tag{3}$$

where Z_i represents Zernike polynomials. The y-field is set 6°~8° about twice of the original system. In the optimizing process the surface figures of the PM and the TM are kept invariant because they can be applied directly in future experiments as ready-made components. Hence the surface figure of FM is optimized as extended polynomial surface with few terms for better aberration balancing and correction. It should be pointed out that if secondary mirror is considered as free-form surface from the initial design stage, there is no need to make any change to the plane FM and good result with the same technical specification (F number, effective focal length, etc.) can be obtained, which has been validated by actual optical design. It can be observed that the final design result of the field-extended system shown in Fig.4 is even a little better than the original system after some optimization in Zemax. Thus, the image plane can be enlarged as twice wide as before, as shown in Fig.5. Four lines of CCD arrays can be arranged in the enlarged image plane as Fig.6 shows: two of them are located at the best-focus position for normal image while the other two are located with fixed defocus for "diversity image", as shown is Fig.7.

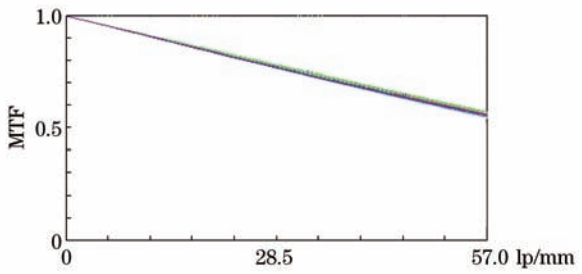

Fig.4 MTF curves of improved system

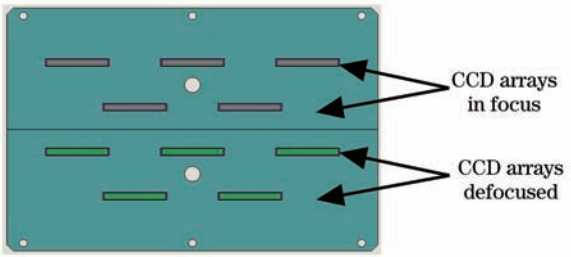

Fig.5 Re-designed image plane

Although the normal image and the "diversity image" are not obtained absolutely simultaneously, the little difference Δt can be ignored without any inaccurate effect considering the extremely rapid velocity of the satellite. Thereby, the two pieces of images can be regarded as being obtained quasi-

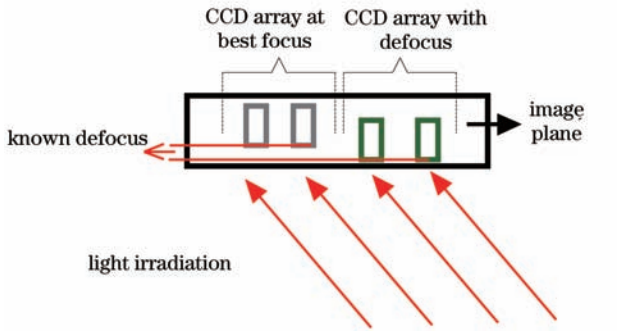

Fig.6 Side elevation of the image plane with PD technology

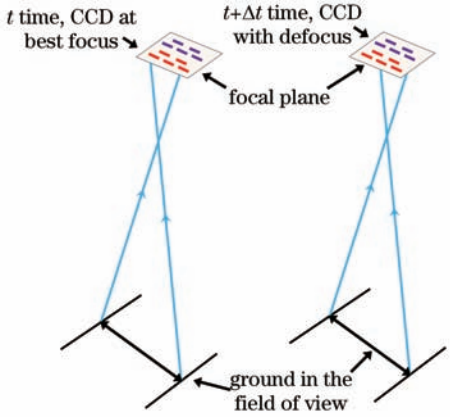

Fig.7 Working mode of PD technology

simultaneously.

The practical experiment was performed by the telescope mentioned above. Two images of the same target were captured, as shown in Fig.8: one is in-focus and the other is set as diversity image in which 0.6 mm defocus is introduced to the focal plane. It should be pointed out that the position of nominal best focusing plane is not important, but the introduced defocus amount between the in-focus image and the diversity image is the most concerned about. The actual defocus amount of the in-focus image can be calculated by PD algorithm. The push-broom imaging was realized by matching the angular velocity of the carrier of telescope and the line transfer frequency of CCD. Two 128 pixel×128 pixel sub-images were extracted from the original images for data processing. The calculating result shows that the deviation of low-spatial-frequency wavefront error between the PD algorithm and interferometric result is lower than 5% and the defocus amount of the nominal in-focus image is 0.72 mm, which agrees with the actual focusing adjustment of 0.7 mm.

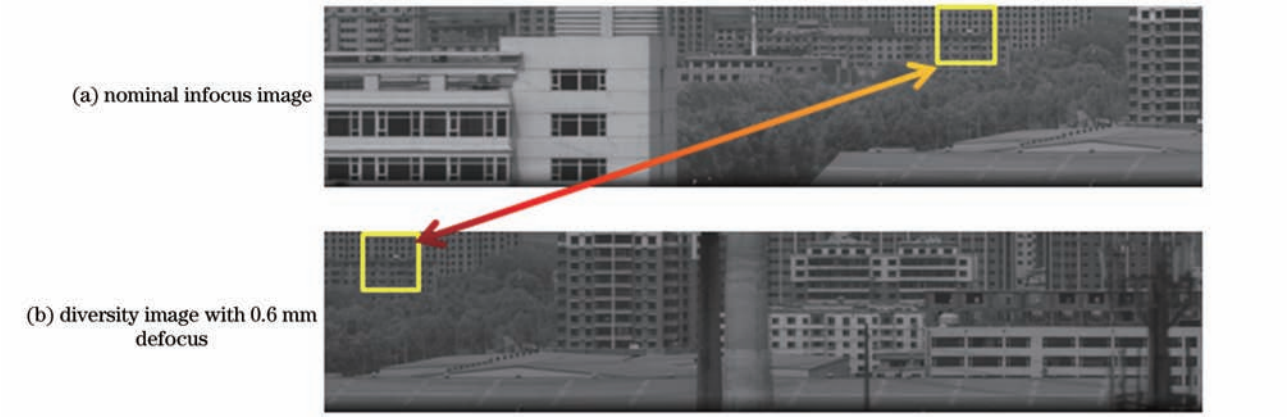

Fig.8 (a) In-focus image and (b) defocus image acquired by PD technology

4 Deformable mirror technology

The active optics technology for space telescope is not a fresh topic, which has been applied on several space optical systems such as Hubble Space Telescope (HST)[15-16]. However, it will be greatly costly and hard to control accurately if all the mirrors are made active especially when the mirror is large (the diameter of the primary mirror of HST is 2.4 m). Furthermore, the telescopes for astronomical application are always energy-collecting system, of which the FOV is very narrow and the target can be regarded as point far away infinitely. Thus the wavefront error can be easily tested by traditional methods such as Shack-Hartmann sensor, obtaining the wavefront-correcting criteria of active loop. Unfortunately, the optics on space-borne camera is imaging system whose mission is to shoot the various objects on ground as clearly and sharply as possible with the lowest cost. Therefore, the wavefront error cannot be detected by traditional wavefront sensing technology while the PD technology referred to above seems a feasible metrology. Because the stop of the off-axis TMA system

under research is located at the secondary mirror, the wavefront from any object in any FOV can be modulated by transforming its surface figure. Thus, most dynamic wavefront errors can be eliminated when only the single secondary mirror rather than all the three mirrors is made active element, which greatly decreases the cost and difficulty. For example, when there is 0.25λ root-mean-square (RMS) astigmatism because of the surface deformation of primary mirror, the wavefront map is shown in Fig.9. After corrected by transforming the surface figure of secondary mirror actively, the residual wavefront error is decreased to 0.03λ (RMS). It can be noticed from Fig.10 that the surface transformation of the secondary mirror has no discontinuity and there is no sharp edge or deep cavity in the surface. Thus, the transformation can be achieved by nano-drivers arranged reasonably.

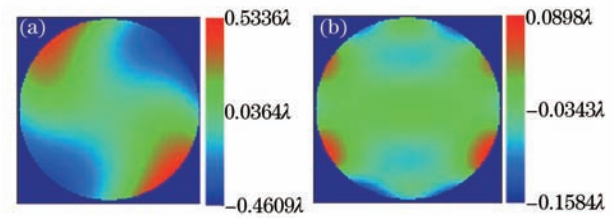

Fig.9 (a) Aberrated wavefront; (b) corrected wavefront

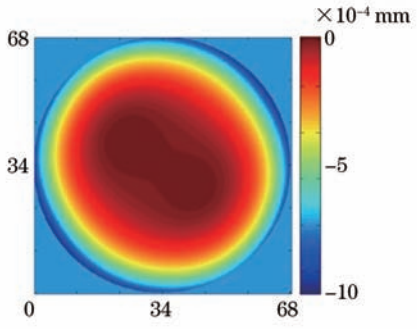

Fig.10 Transformation of surface figure of the secondary mirror

It is extremely difficult to manufacture a deformable mirror with convex asphere figure, so firstly our group made a practical deformable plane mirror and performed the experiment of correcting wavefront error of the telescope mentioned above. The deformable mirror was located in the optical path of the telescope and was used as a folded mirror, as shown in Fig.11. The wavefront error of one

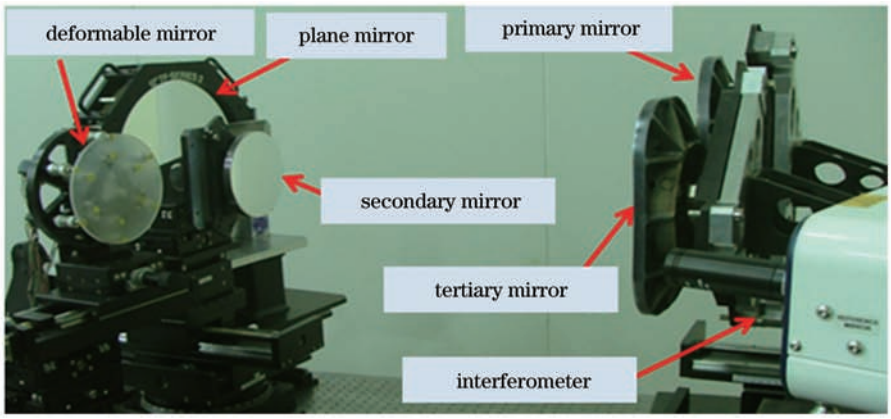

Fig.11 Experimental setup of correcting wavefront error by deformable mirror

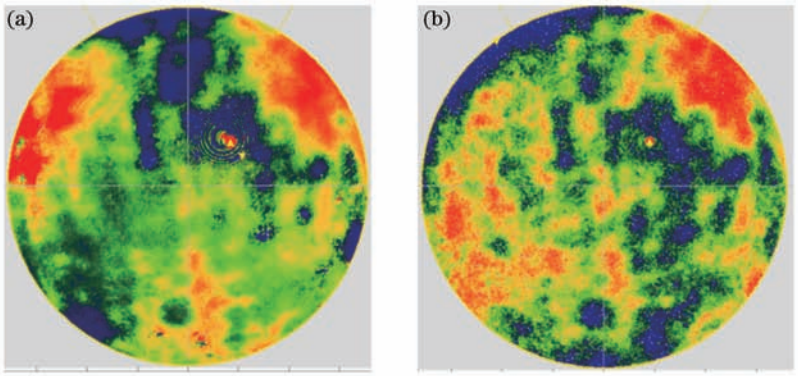

Fig.12 Wavefront maps (a) before and (b) after correction

FOV can be corrected. It can be seen from Fig.12 that the wavefront error is 0.122λ(RMS, λ=632.8 nm) before correction and it decreases to 0.0879λ(RMS) after correction, and the trefoil error is eliminated basically.

5 Conclusion

For an off-axis TMA system, the possibility and advantages of so-called intelligent pupil technology which improves optical performance by manipulating the surface figure of secondary mirror are discussed. Some research has been developed: 1) The secondary mirror with cubic terms shown in Eq.(3) for wavefront coding system has been polished; the manufacturing and testing of this unusual asphere will be described later. 2) The preparation of fabrication of another secondary mirror with free-form addition has been made, which is scheduled to be polished after the accomplishment of the secondary mirror with cubic terms. The new image plane with extra CCD arrays as shown in Fig.6 is also designed in detail. 3) The basic form of the active secondary mirror is considered to be thin mirror with nano-drivers supporting its back; the arrangement of nano-drivers has been designed and the structure of nano-drivers is under investigation. It is arranged the last step of our experiments. All the three new kinds of secondary mirror are planned to be assembled in the TMA system and the performance improvement will be verified by actual imaging experiments.

Reference

1 Wetherell W B, Womble D A. All-Reflective Three-Element Objective: US, 4240707 [P]. 1980-12-23.

2 Alan R FitzGerrell, Edward R Dowski, W Thomas Cathey. Defocus transfer function for circularly symmetric pupils [J]. Appl Opt, 1997, 36(23): 5796-5804.

3 Sara Bradbum, Wade Thomas Cathey, Edward R Dowski. Realizations of focus invariance in optical-digital systems with wave-front coding [J]. Appl Opt, 1997, 36(35): 9157-9166.

4 Feng Yan, Ligong Zheng, Xuejun Zhang. Design of an off-axis three-mirror anastigmatic optical system with wavefront coding technology [J]. Opt Eng, 2008, 47(6): 063001.

5 Sean Quirin, Darcy S Peterka, Rafael Yuste. Instantaneous three-dimensional sensing using spatial light modulator illumination with extended depth of field imaging [J]. Opt Express, 2013, 21(13): 16007-16021.

6 Jeffrey A Davis, Don M Cottrell. Effects of the optical system on the output from wavefront coding masks [J]. Opt Express, 2011, 19(18): 17677-17682.

7 Vikrant R Bhakta, Manjunath Somayaji, Marc P Christensen. Applications of the phase transfer function of digital incoherent imaging systems [J]. Appl Opt, 2012, 51(4): A17-A26.

8 J J Dolne, R J Tansey, K A Black, *et al*.. Practical concerns for phase diversity implementation in wavefront sensing and image recovery [C]. SPIE, 2002, 4493: 100-111.

9 David J Lee, Michael C Roggemann, Byron M Welsh, *et al*.. Evaluation of least-squares phase-diversity technique for space telescope wave-front sensing [J]. Appl Opt, 1997, 36(35): 9186-9797.

10 Gregory C Dente, Michael L Tilton. Segmented mirror phasing using the focal-plane intensity [J]. Appl Opt, 2012, 51(3): 295-301.

11 C S Smith, R Marinică, A J den Dekker, *et al*.. Iterative linear focal-plane wavefront correction [J]. J Opt Soc Am A, 2013, 30(10): 2002-2011.

12 Peter Kner. Phase diversity for three-dimensional imaging [J]. J Opt Soc Am A, 2013, 30(10): 1980-1987.

13 Paolo Spanò. Free-forms optics into astronomical use: The case of an all-mirror anamorphic collimator [C]. SPIE, 2008, 7018: 701840.

14 Warren J Smith, Ellis Betensky, David Williamson, *et al*.. The past, present, and future of optical design [C]. SPIE, 2006, 6342: 63422Y.

15 Jim H Burge. Ultra-lightweight, actively controlled mirrors for space [C]. SPIE, 1999, 3749: 84-85.

16 R Arsenaulta, R Biasib, D Gallienic, *et al*.. A deformable secondary mirror for the VLT [C]. SPIE, 2006, 6272: 62720V.